05

The effect of chemical-mechanical processing of silicon wafers on their surface morphology and strength

© V.A. Kozlov,[1,2] V.I. Nikolaev,[1] V.V. Shpeizman,[1] R.B. Timashov,[1] A.O. Pozdnyakov,[1] S.I. Stepanov[1]

[1] Ioffe Institute, St. Petersburg, Russia
[2] AO „PK FID-Tekhnika", St. Petersburg, Russia
e-mail: shpeizm.v@mail.ioffe.ru

The mechanical strength of various silicon wafers with a thickness of 100μm has been studied, depending on the methods of their preparation and the modes of their subsequent grinding or polishing, including chemical-mechanical (HMP). The plates were loaded using the ring-to-ring method, the magnitude of stresses and deflection under the small ring was determined by the finite element method. For all the samples studied, the profiles and roughness parameters of the plates were obtained by stylus profilometry and atomic force microscopy (AFM) when scanning the surface along the baseline and over the area. A direct correlation was found between the strength of the plates and the characteristic parameters of their surface profile (the average values of the magnitude and period of fluctuations in the height of the irregularities).

Keywords: silicon wafer, strength, chemical-mechanical polishing treatment, surface morfology.

Introduction

Thin and ultrathin silicon wafers for modern electronics are considered to be plates of relatively large diameter D (more than 100 mm) and small thickness d, the value of which satisfies the condition $d < 0.001D$. The main consumers of silicon wafers with a thickness of 100μm or less are manufacturers of MEMS systems and CMOS sensors, devices $3D$-memory and ultra-bright LEDs, power and microwave electronics devices, as well as photovoltaic converters for solar energy. The need to use increasingly thin plates is determined by the desire of manufacturers to reduce the material consumption of chip production and improve the totality of their operational characteristics. The task of reducing the thermal resistance of instrument structures, which is directly related to a decrease in their thickness should be specifically noted. Currently it is thermal effects to a large extent that limit the limiting parameters of the operation of most semiconductor electronics devices. With a decrease in the thickness of semiconductor structures, the mechanical strength of both the initial plates as a whole and the chips themselves becomes extremely important. The strength of the initial material of the plates and finished chips significantly affects the amount of manufacturing defects, the percentage of yield of suitable devices and their reliability, as it determines the resistance of the material to possible damage to the plates and chips both during their manufacture and assembly, and during operation as a result of various thermomechanical influences (thermal shocks and thermal cycling, vibration, shock loads, sharp accelerations, etc.).

In connection with the above, the topic of mechanical strength of silicon thin plates has been of increased interest in recent years. It should be noted that various aspects of this problem are discussed in the literature — from methods for obtaining silicon itself and processing the surface of silicon wafers, to choosing the type of loading of samples, methods for calculating stresses and finding the strength limit of wafers, as well as the relationship between the electrical, optical and mechanical properties of wafers with different roughness and its structure surfaces.

In this work, the strength was determined and the structure and morphology of the surface of differently prepared thin silicon wafers were investigated, and an attempt was made to link the strength value with the method of obtaining, processing and characteristics of the surface roughness of the wafers.

1. Samples and methods of strength measurement

1.1. Preparation of samples

Table 1 presents all types of tested samples indicating the origin, composition and methods of surface treatment of single-crystal silicon wafers. In total, 9 groups were prepared for testing, each of which had from 10 to 20 samples. In lines $1-4$ of the table, data are given for silicon p-a type of conductivity grown using the Czochralski method, doped with an acceptor admixture of boron to the level of $N_A = 5 \cdot 10^{18}$ or 10^{19} cm^{-3} with a resistivity value of ~ 5 and $10 \mu\Omega \cdot$ cm respectively. The initial plates with an orientation of (100) with a diameter of 100 mm and a thickness of 420μm were subjected to one-sided high-quality factory two-stage chemical-mechanical

Table 1. Preparation characteristics and strength of silicon wafers

№ of group	Type of Si plates, Thinning Mode	Finishing Mode	Strength, MPa
1	p-Si (100) — Czochralski (Russia), $N_A = 5 \cdot 10^{18}\,\text{cm}^{-3}$. M14 Powder Grinding+AFM+CMP Polishing	CMP-2	1010 ± 456
2	p-Si (100) — Czochralski (China), $N_A = 1 \cdot 10^{19}\,\text{cm}^{-3}$. M14 Powder Grinding+AFM+CMP Polishing	CMP-2	989 ± 440
3	p-Si (100) — Czochralski (Russia), $N_A = 5 \cdot 10^{18}\,\text{cm}^{-3}$. M14 Powder Grinding+AFM+CMP Polishing	CMP-1	616 ± 318
4	p-Si (100) — Czochralski (China), $N_A = 1 \cdot 10^{19}\,\text{cm}^{-3}$. M14 Powder Grinding+AFM+CMP Polishing	CMP-1	695 ± 340
5	p/n-Si (100) — epitaxy (Russia), p-Si $(50\,\mu\text{m})$+n-Si $(50\,\mu\text{m})$, p-Si(B) c $N_A = 2 \cdot 10^{14}\,\text{cm}^{-3}$, n-Si(100) c $N_D = 1 \cdot 10^{14}\,\text{cm}^{-3}$ M14 Powder Grinding+AFM+CMP Polishing	CMP-2	754 ± 506
6	p/n-Si (100) — epitaxy (Russia), p-Si $(50\,\mu\text{m})$+n-Si $(50\,\mu\text{m})$, p-Si(B) c $N_A = 2 \cdot 10^{14}\,\text{cm}^{-3}$, n-Si(100) c $N_D = 1 \cdot 10^{14}\,\text{cm}^{-3}$ M14 Powder Grinding+AFM+CMP Polishing	CMP-1	482 ± 246
7	p/n-Si (100) — epitaxy (Russia), p-Si $(50\,\mu\text{m})$+n-Si $(50\,\mu\text{m})$, p-Si(B) c $N_A = 2 \cdot 10^{14}\,\text{cm}^{-3}$, n-Si(100) c $N_D = 1 \cdot 10^{14}\,\text{cm}^{-3}$ M14 Powder Grinding+AFM polishing	Diamond polishing AFM 3/5	152 ± 59
8	n-Si (100) — Czochralski (China), $N_D = 1 \cdot 10^{15}\,\text{cm}^{-3}$. Grinding with powder M7	Grinding with powder SiC M7	144 ± 33
9	n-Si (100) — Czochralski (China), $N_D = 1 \cdot 10^{15}\,\text{cm}^{-3}$. Grinding with powder M14	Grinding with powder SiC M14	127 ± 13

polishing (CMP) and brought to a thickness of $100\,\mu\text{m}$ with the same diameter. These procedures were carried out in several stages by grinding the back side of the plates: (1) free abrasive with grain size of the main fraction $14\,\mu\text{m}$ to thickness $200\,\mu\text{m}$, (2) diamond pastes with grain $5/3\,\mu\text{m}$ to thickness $130\,\mu\text{m}$, (3) diamond paste with grain $1\,\mu\text{m}$ to thickness $110\,\mu\text{m}$, (4) finishing CMP plates with thickness $100\,\mu\text{m}$ were obtained.

The samples were ground and polished with diamond pastes in JSC PK „FID-Tekhnika" using the equipment produced by „PeterWolters GmbH". 500 mm glass grinding wheels were used for gridning, the rotation speeds of the wheels and plates were ~ 20 and $10\,\text{min}^{-1}$, respectively; hold-down pressure $\sim 50\,\text{g/cm}^2$. Polishing was performed using polishing machines „Unipol-1202" with 300 mm polishing wheels „Simba-N" manufactured by „MetCata GmbH". The plates were polished in a suspension of diamond powder AFM 5/3 in a mixture of synthanol and glycerin with a ratio of 1,:,50. The rotation speeds of the polishing wheel and the plate were respectively about 100 and $20\,\text{min}^{-1}$, hold-down pressure $80-100\,\text{g/cm}^2$. A suspension of pyrogenic silicon dioxide in KOH or ethylenediamine with $\text{pH} = 10-12$ was used for CMP. Chemical-mechanical polishing was carried out on „Unipol-1202" machines with polishing wheels „Simba-N" at a rotation speed of the wheel of the order of $200\,\text{min}^{-1}$ and pressure $250-350\,\text{g/cm}^2$. At the first stage of polishing

(CMP-1), a suspension of silicon dioxide nanoparticles with a size of $10-40\,\text{nm}$ in an amount of $10-20\,\text{wt.\%}$ was used, which ensured the final removal of a layer of material with a thickness of $\sim 25-30\,\mu\text{m}$. The second stage (CMP-2) was carried out using nanoparticles of amorphous SiO_2 with a size of $7\,\text{nm}$, and the rotation speed of the polishing wheel and the pressure value decreased to $\sim 80\,\text{min}^{-1}$ and $\sim 100\,\text{g/cm}^2$, respectively. The use of the finishing polishing described above, developed by JSC „Gyrooptics", led to a significant reduction in the rate of removal of the plate material and ensured the achievement of a smoother surface of silicon wafers. The thickness of the silicon layer removed at the second stage of finishing polishing usually did not exceed $3-5\,\mu\text{m}$.

Silicon plates in the first 4 rows of Table. 1 have different manufacturers, differ in the impurity content and the type of finishing polishing (HMP-1 or HMP-2). In lines $5-7$ Table 1, samples of monocrystalline silicon obtained by epitaxial accretion of layers p- and n-type of conductivity with a thickness of $50\,\mu\text{m}$ on the same the original substrates that were described above. Epitaxial growth processes were performed in LPE's PE2061S epitaxial growth plants at the production facilities of JSC „Epiel". Doping of epitaxial layers p-type of conductivity with acceptor impurity (boron) and layers n-type of conductivity with donor impurity (phosphorus) was of the order of $2 \cdot 10^{14}\,\text{cm}^{-3}$. Reducing the thickness of the plates to $100\,\mu\text{m}$ was achieved by

completely removing the substrate by grinding-polishing methods similar to the modes described above. Samples in lines $5-7$ table. 1 differ in finishing polishing: CMP-1, CMP-2 and diamond powder. In lines 8, 9 of Table 1, the results are given for samples of electronic-type silicon grown using the Czochralski method and doped with phosphorus to the level of $N_D = 1 \cdot 10^{15}\,cm^{-3}$ with a resistance of $5\,\Omega\mu \cdot cm$ (the so-called „solar" silicon). The initial plates had the shape of „pseudo-squares" with $125\,mm$ side, thickness $180\,\mu m$ and orientation (100). Plates with a diameter of $100\,mm$ were cut out of initial plates, then they were ground to a final thickness $100\,\mu m$. At the same time, layers of equal thickness ($\sim 40\,\mu m$) were removed from each side of the plates until reaching the final thickness of $100\,\mu m$. SiC grinding powder with the grain size of the main fraction 14 and $7\,\mu m$ was used for grinding.

The samples for strength tests had the shape of disks with a diameter of $11.8\,mm$, were cut with a fiber pulsed laser „MiniMarker 2" with a wavelength of radiation $1.06\,\mu m$ in ablation mode. The temperature of the silicon wheels after the end of the cutting process was recorded using a thermal imager of the brand „Ti32 ThermalImager" manufactured by „FlukeCorp". The presence of thermomechanical stresses and the thickness of the disturbed silicon layers adjacent to the cut area were monitored according to X-ray topography using the Lang method in the reflection of $(531)\,CuK_\alpha$ at $\alpha = 30°$, $2\theta = 114°$. Selected cutting mode (pulse duration $12-30\,ns$, average light power $5-10\,W$, pulse repetition rate $20-40\,kHz$, light spot movement speed $400-800\,mm/s$) provided a temperature of no more than $100°$ in the cutting area and the thickness of the layers disturbed by cutting of $\sim 10\,\mu m$.

Measurements of the thickness of the samples were carried out with an accuracy no worse than $1\,\mu m$, which was achieved by using a digital linear displacement converter with a rod „LIR-19A", a digital display device „LIR-500A" and a measuring optical rack „C-III M" with table. The spread of the thickness of individual wheels within their diameter of $11.8\,mm$ did not exceed $1\,\mu m$, the spread of the average thickness of $11.8\,mm$ wheels in the groups selected for measurements was $\pm 2\,\mu m$.

1.2. Test procedure and stress calculation

Many papers have been published in recent years on the strength of silicon wafers. There is currently no single criterion for choosing a method for determining the strength of thin silicon wafers. Most researchers take the critical maximum tensile stress during bending, uniaxial (three- or four-point uniaxial bending of strips [1–8]) or biaxial (biaxial) bending of plates as the strength value [9–14]. Other types of impacts are used much less frequently, for example, indentation of [15] and destruction as a result of thermal expansion during heating, stimulating the development of cracks [16]. Analytical expressions for maximum bending stresses were borrowed from the work on the destruction of other brittle bodies (glass, ceramics,

etc.). The strength is calculated according to the formulas of the classical theory of elasticity in accordance with the standard ASTMC 1161-02c for the case of uniaxial bending with ASTM C 1499–15 for an axisymmetric variant of biaxial bending, the stress and deflection formulas for which, used in experiments, were first obtained and applied to glass in Ioffe Institute [17]. The disadvantage of analytical solutions for bending stresses is that they work with small deflections, which is true for thin silicon wafers only for samples with low strength [13].

The use of the finite element method (finite element method, FEM) [1,9,11–14] has opened up wide possibilities for analyzing the stress state of plates of any strength. This fully applies to both single- and biaxial bending. The created programs made it possible to calculate stresses at large deflections for uniaxial bending [1], as well as to use various combinations of the shape of the support and loading devices during biaxial bending, such as ring-in-ring (ring-on-ring test) [1,9,11–14], ball-b-ring (ball-on-ring test) [18], rod-in-ring, (piston-on-balls test), ball-in-3 balls, which are the vertices of an equilateral triangle (ball-on-three-balls test) and 3 balls-in-3 balls with the largest distance between the support balls (three-balls-on-three-balls test). It should be noted that only the first two types of support and loading device combinations were used for silicon, the rest were used for ceramic samples [19]. However, tests with three balls may also be of interest for silicon, since the problem of determining stresses for them is not axisymmetric, as in other cases, which is the case for most crystallographic directions in single crystals of silicon. Elastic constants in silicon single crystals are isotropic only in the planes (111), which makes it necessary to use a certain averaged modulus of elasticity [13] when determining stresses.

Ring-to-ring method, i.e., ring supports and a loading tip are used, is the most common method of loading for measuring the strength of thin silicon wafers by biaxial bending. At the same time, the dimensions of the plate exceed the diameter of the large ring, so that its edges, which are obvious stress concentrators, protrude beyond the support, turn out to be weakly loaded and cannot be the nuclei of a crack leading to destruction. When the strips are stretched by a three- or four-point bend, destruction in most cases begins at the edge of the plate. Calculations of stresses by the finite element method for ring-to-ring loading and their direct measurement by X-ray or optical methods [11,20,21] showed that the maximum radial stresses are at the points of the surface under the ring of smaller diameter on the side of the plate opposite to the side of contact of this ring. Tangential stresses also have a maximum at these points, but their magnitude is noticeably smaller than radial ones. It should be noted that the actual stresses in thin plates during the ring-to-ring test may differ slightly from those calculated for the axisymmetric bending problem. The reason for this may be contact stresses (the stress field in the Hertz contact problem), the asymmetry of the elastic properties of the plate material mentioned above, which occurs, for example, in silicon orientation [100]),

as well as various kinds of asymmetry of the surface morphology and etc.). Since the direct determination of stresses is a very difficult task, the question arises about the control of computational methods for determining stresses. In the present work, a simple method was used to evaluate the correctness of the computational model in comparison with the dependence obtained in it of the deflection value under a small diameter ring on the load with a similar dependence of the experimental deflection, which is equal to the displacement of the movable rod of the testing machine.

The strength of wafers was determined using „Instron1342“ multi-purpose testing machine with an attachment for axially symmetric bending designed at the Ioffe Institute. A set of support and loading rings with a diameter of 8.4 and $4.4\,\mu$m, respectively, was fabricated for testing the strength of samples with a diameter of 11.8mm and a thickness of $100\,\mu$m. The loading rate was 0.2 mm/min. The force of F was recorded during the experiment depending on the movement of the rod of the testing machine $\Delta l = w(a)$, i.e., the deflection of the plate under the loading ring. The problem of determining the maximum stresses σ as a function of the applied force F was discussed in detail in [13], both experimental and numerical methods were considered. It was shown that stress calculations by the finite element method ensure a good match with the well-known experiment. Calculations were performed using „Comsol Multiphysics“ package in this study. An axisymmetric plate model using rectangular finite elements and a characteristic cell size approximately 4 times smaller than the plate thickness was considered. As boundary conditions, the following were set: absence of movements along the perimeter of the contact of the support ring and the plate and uniform distribution of the load along the perimeter of the contact of the loading ring and the plate. The model used ensured a good convergence of the solution. The criterion for the correctness of the stress calculation was a comparison of the experimental dependence of the load F on the deflection $w(a)$, where a — the radius of the small ring with the obtained FEM under the same boundary conditions that were used in the stress calculation. Figure 1 shows the curve $F\big(w(a)\big)$ averaged over 125 samples with different surface treatment, but unchanged test geometry, and the calculated curve. Fig. 1 shows that the calculated and experimental curves are close, which makes it possible to determine the maximum stresses in the plate according to the dependence $\sigma(F)$ obtained in the framework of the calculation described above (Fig. 1). The material characteristics of nine groups of samples and their mechanical strength, for which the average value was taken the calculated values of radial stresses at the moment of destruction are given in Table. 1.

The surface profilometry of the samples was carried out using a stylus profilometer „AlphaStepD120“ manufactured by „KLA-TencorCorp“. The surface structure of the samples was monitored using an optical microscope „Nikon Eclipse“, as well as a scanning electron microscope
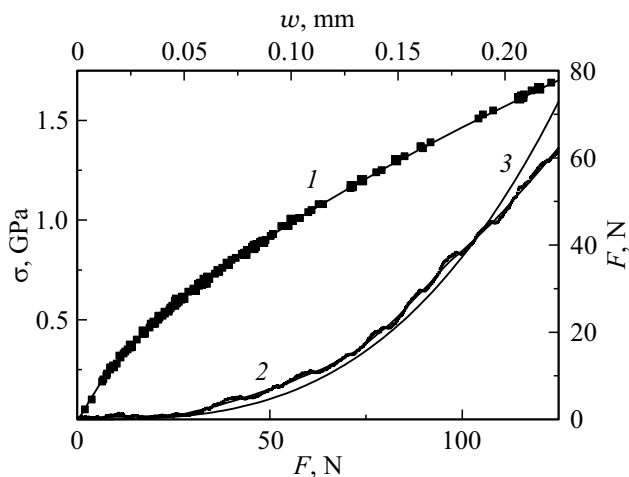

Figure 1. The ratio between the applied force F and (*1*) stresses σ (scale lower and left, curve — calculation using FEM, points — samples for samples with different strength) and between F and the deflection under the small ring w (*2* — experiment, *3* — calculation using FEM).

„Camscan S4-90FE“ („Cambridge Instruments“). The atomic force microscope „NTEGRA Aura“ produced by „NT-MDT“ was used for a detailed study of the surface of samples on a nanometer scale.

2. Measuring the strength of samples

Despite the large variation in the strength values of silicon wafers, which is typical for brittle bodies, a comparison of the average strength values of differently prepared samples reveals the following trends in its changes depending on the type of plate and finishing treatment (Table 1). The lowest strength value was shown by samples that were treated only by grinding with a free abrasive with grain size the main fractions are 14 and $7\,\mu$m (127 and 144 MPa, respectively, the bottom two rows of the table). Samples from p-type crystals grown using the Czochralski method after two-stage CMP (CMP-1 + CMP-2) had higher strength compared to samples processed only in one stage of CMP-1 ($\sim$ 1 GPa vs. 0.6 GPa). At the same time, the difference in the strength of silicon from different manufacturers with a slightly different level of boron doping was no more than 10%. For epitaxially grown silicon layers, the plates after two-stage polishing also had an average strength that exceeded the strength achieved during the one-stage process (0.75 GPa vs 0.48 GPa). Such an effect of differences in polishing on the strength of brittle bodies of various nature (semiconductors, glasses, ceramics, etc.) is well known and is usually associated with the fact that finishing polishing (CMP-2) with weak mechanical action and a more pronounced component of the chemical process of removing the material smoothens the surface irregularities remaining after the first stage of CMP-1 polishing. At the same time, for the first stage of the polishing process, even if
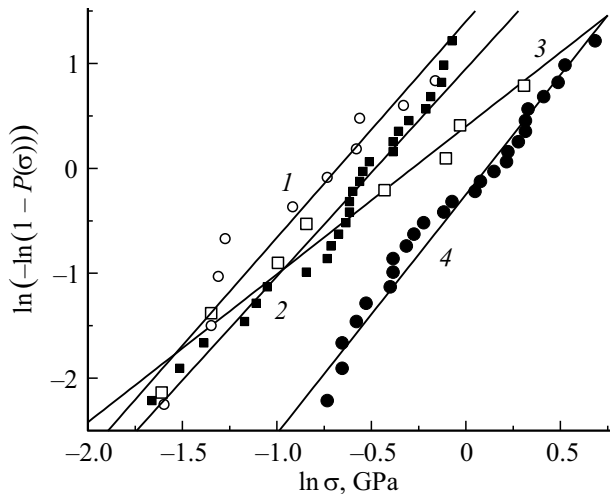
Figure 2. Weibull distributions for epitaxial silicon $(1, 3)$ and grown using the Czochralski method $(2, 4)$ after finishing HMP-1 $(1, 2)$ and HMP-2 treatment $(3, 4)$.

Table 2. Characteristics of the Weilbull distribution for the strength of epitaxial and Czochralski-grown silicon

Silicon production method	CMP-1		CMP-2	
	m	σ_0, GPa	m	σ_0, GPa
Epitaxy	2.06	0.50	1.41	0.76
Czochralski	1.98	0.63	2.28	1.11

irregularities remain after it, small in height, they have sharp peaks and are dangerous stress concentrators, which reduces the strength of samples with such a surface.

It follows from the data given in the table that the method of obtaining silicon (epitaxial or grown using the Czochralski method) affects the strength of the samples, and small differences in the degree of doping of the studied crystals with boron from different manufacturers practically do not affect their strength. The difference for samples with different doping did not exceed the accuracy of the measurements performed and was noticeably lower than the level of dispersion of the strength values of samples from the same group.

The Weibull distribution $P(\sigma)$, which has the form provided below is usually used for the analysis of the scattering of strength measurements of silicon, as well as other brittle materials [20]:

$$P(\sigma) = 1 - \exp\left(-\left(\frac{\sigma}{\sigma_0}\right)^m\right), \qquad (1)$$

where two parameters σ_0 and m characterize, respectively, the strength and the width of its distribution. An experimental dependence is constructed in the coordinates $\ln\left(-\ln(1-P)\right) - \ln\sigma$ to determine these parameters. This dependence is a straight line which according to (1)

with slope is m, and σ_0 can be calculated using another parameter. Similar dependencies are shown on Fig. 2 as an example for samples p^+-Si, obtained using the Czochralski method (rows 1−4 Table 1, data for silicon from different manufacturers were combined) and epitaxial samples (lines 5 and 6 tables. 1), exposed to CMP-1 and (XMP-1 + CMP-2). The values of the Weibull parameters are given in Table. 2. The straight lines drawn from experimental points have a small slope and are shifted along the stress axis, which indicates a different strength value and a slightly different distribution width. The small value of m is obviously related not only to the natural variation in the strength value, but also to the small size of the samples, for which small deviations under loading conditions can lead to large changes in it.

It should be noted that the Weibull distribution alone, based on the concept of the weakest link and fair in the case of determining the strength when loading a sample at a constant speed, may not be enough to predict the service life of silicon wafers in real conditions. As it was shown in [21], the presence of a cyclic component of the load, which occurs, for example, with temperature fluctuations or vibration, leads to an acceleration of destruction. These effects can be most pronounced, for example, for power electronics devices and MEMS. Thus, the kinetic effects should be taken into account when predicting the destruction of crystals of silicon-based semiconductor devices.

3. Investigation of the morphology of the surface of samples

The height of irregularities on the surface of silicon samples grown using the Czochralski method, after CMP-1 and CMP-2 along the baseline was measured to establish the relationship of strength with the characteristics of the surface profile (Fig. 3). There are also curves averaged over 50 points with clearly traced the periodicity of the height of the points of the surface profile. The surface roughness was estimated using the following parameters: the average value of the absolute values of the profile height R_a, the difference between the maximum and minimum values of the height $R_Y = R_{max} - R_{min}$, the height of the profile irregularities at 10 points (5 the largest and 5 the smallest) R_z, the standard deviations of the measured height values R_q and their deviations from the averaged curve R_{qs}, as well as the step of irregularities on the averaged curve (Table 3). As can be seen from Table. 3, all parametres of the height of irregularities for samples after CMP-1 are higher than for samples after CMP-2, and the pitch of irregularities is less.[1] The results obtained are obviously related to the influence of the chemical component of polishing, which prevails in CMP-2,

---

[1] It should be noted that in order to determine the small steps of changes in the height of the profile, it is necessary to carry out a larger number of measurements, as well as to consider the possible impact of various kinds of interference on them.

Table 3. Surface roughness characteristics measured along the baseline

Roughness Characteristic	CMP-1	CMP-2
Average value of absolute profile height values R_a, nm	0.47	0.26
The difference between the maximum and minimum profile height $R_{max} - R_{min}$, nm	2.89	1.60
Height of profile irregularities over ten points R_z, nm	2.83	1.54
Standard deviation R_q, nm	0.61	0.34
Standard deviation from the averaged curve R_{qs}, nm	0.43	0.24
Irregularity pitch S_m, μm	0.44	≈ 4.2
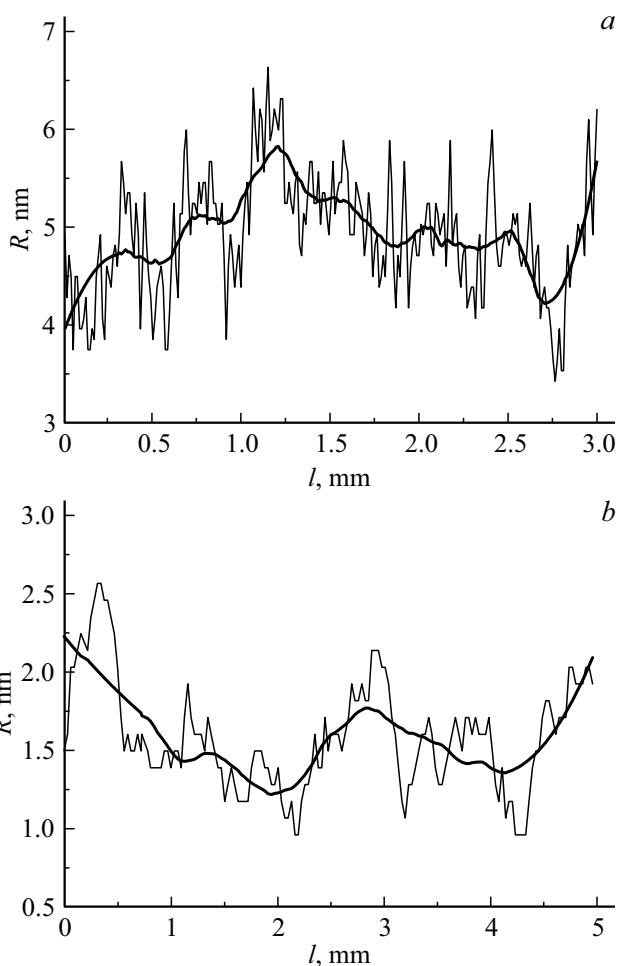
Figure 3. Dependence of the height of the surface irregularities of the silicon wafer when measured along the line; type of finishing: CMP-1 (*a*), CMP-2 (*b*).

which smooths out irregularities, reducing their height and stretching the irregularities over a longer surface length. The nature of the irregularities also determines the ratio of the strength of the samples, which is lower for the samples after CMP-1 compared to CMP-2 (Table 1).

The above data on the differences in the roughness of the plates measured in the linear mode of recording their surface profile were also confirmed for the case of scanning the surface of the samples by area. Fig. 4 shows examples of such scanning for two groups of samples after polishing in CMP-1 and CMP-2 modes. The results of processing of scans performed similarly to the linear scanning mode are listed in Table 4, which also confirm that polishing in the CMP-2 mode provides lower values of height differences of the surface relief of samples and a lower level of their roughness in comparison with the standard CMP-1 treatment.

When comparing the results of scanning the surface profile by line and by area, it should be noted that the advantage of line measurements is that they have one coordinate along which the height of the surface points is consistently measured. This is important for analyzing the frequency of variations of the height of the surface relief. But the area measurements are more representative based on the number of points. The surface roughness characteristics differ from those along the line, since in the first case there are significantly more measurement points ($\sim 25\,000$ versus ~ 250), and the maximum height spread is greater for both one pair of points and 10 points.

Figure 5, *a* shows an area scan and a typical linear profilogram of the surface of a silicon sample polished with diamond paste with a grain size of $1\,\mu$m (line 7, Table 1). Fig. 5, *b*, c show the structure and surface profile of samples that were ground with powders with abrasive grain size 7 and $14\,\mu$m (lines 8 and 9, Table. 1). Without dwelling in detail on the details of the analysis of experimental data for samples of these groups, it can be stated that their strength also turned out to be directly dependent on the parameters of the roughness of their surface: the more acute and deep
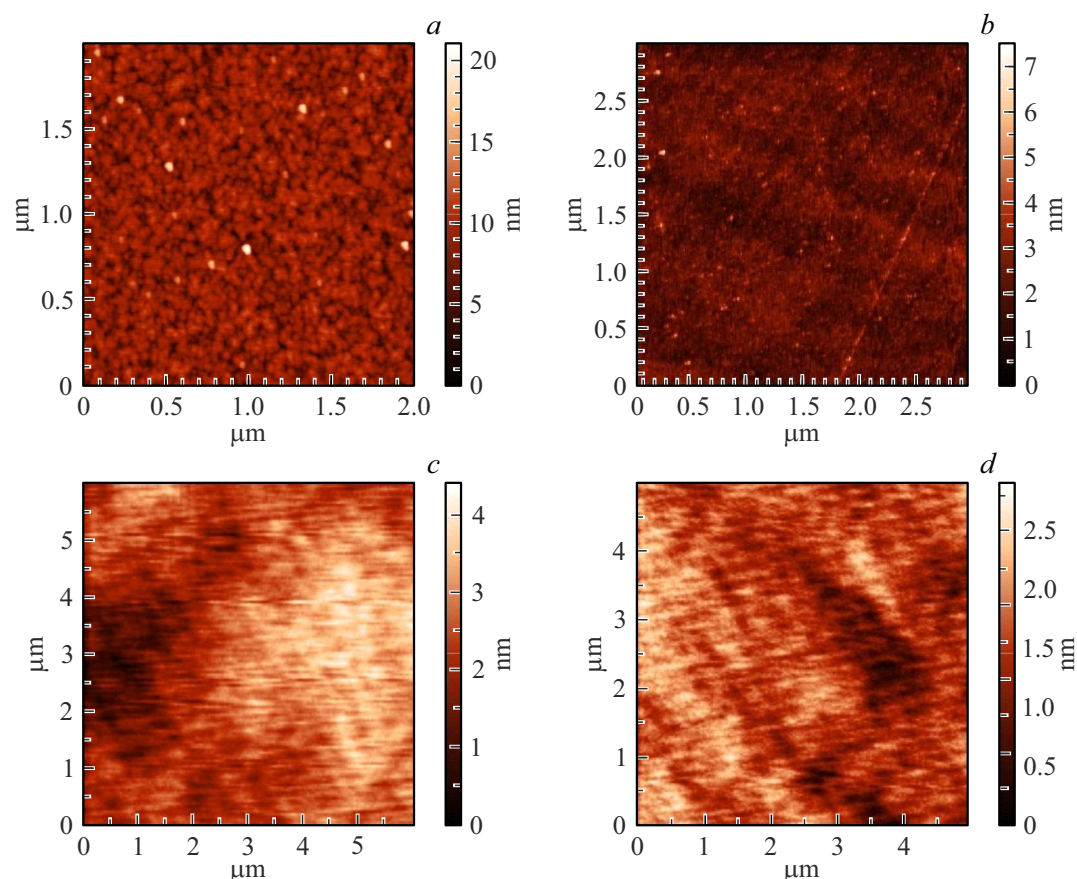
Figure 4. Examples of AFM scans of the surface of four polished silicon wafers grown using the Czochralski method and differing in the polishing mode: scan 1 (*a*) and scan 2 (*b*) — for wafers polished in the CMP-1 mode; scan 3 (*c*) and scan 4 (*d*) — for plates polished in the HMP-2 mode.

violations were present on the surface of the samples, the less their strength turned out to be.

The set of relief heights measured along a certain direction for silicon wafers with different surface treatments can be considered as a manifestation of a random process, the characteristics of which can be determined by direct Fourier transform of the experimentally obtained height dependencies R_n on the point number (distance). A detailed description of the use of the flicker-noise spectroscopy method for analyzing the surface roughness of silicon wafers is given in [22]. [23–25] develop a method of quantitative analysis of the morphology of surface structures formed during deformation and destruction of loaded solids is developed, based on the concept of scale invariance of the surface relief caused by defects [24]. Scale invariance is analyzed on the basis of high-resolution profilometry data and calculation of scaling indicators (fractal dimension and Hurst index [24]). A change in the Hurst parameter for the surface roughness of samples exposed to cyclic or high-speed loading was studied in [26]. A slight change of the Hurst index during fatigue loading of samples and a significant change in it for dynamically loaded samples were found.

Table 4. Surface roughness characteristics averaged from data for two scans of plates with CMP-1 and CMP-2

Roughness Characteristic	CMP-1	CMP-2
Maximum drop peak−depression $R_Y = R_{max} - R_{min}$, nm	11.50	3.64
Height of profile irregularities over ten points R_z, nm	5.65	1.82
Standard deviation R_q, nm	0.69	5.69

Figure 6 shows in double logarithmic coordinates the dependence of the real part of the power spectrum of a random process on the frequency. The Hurst constant H_1 was determined by the formula $n = 2H_1 + 1$ [27]. The values of n and H_1 for silicon wafers with CMP-1 and CMP-2 are given in Table 5. It is concluded in [28] that the parameter H_1 is zero for periodic or close to periodic variations of the observed value, and in [24] it is shown that $H_1 = 0.5$ corresponds to random processes, moreover, for $H_1 < 0.5$, which is the case for both series of our samples, the system retains the property of anti-
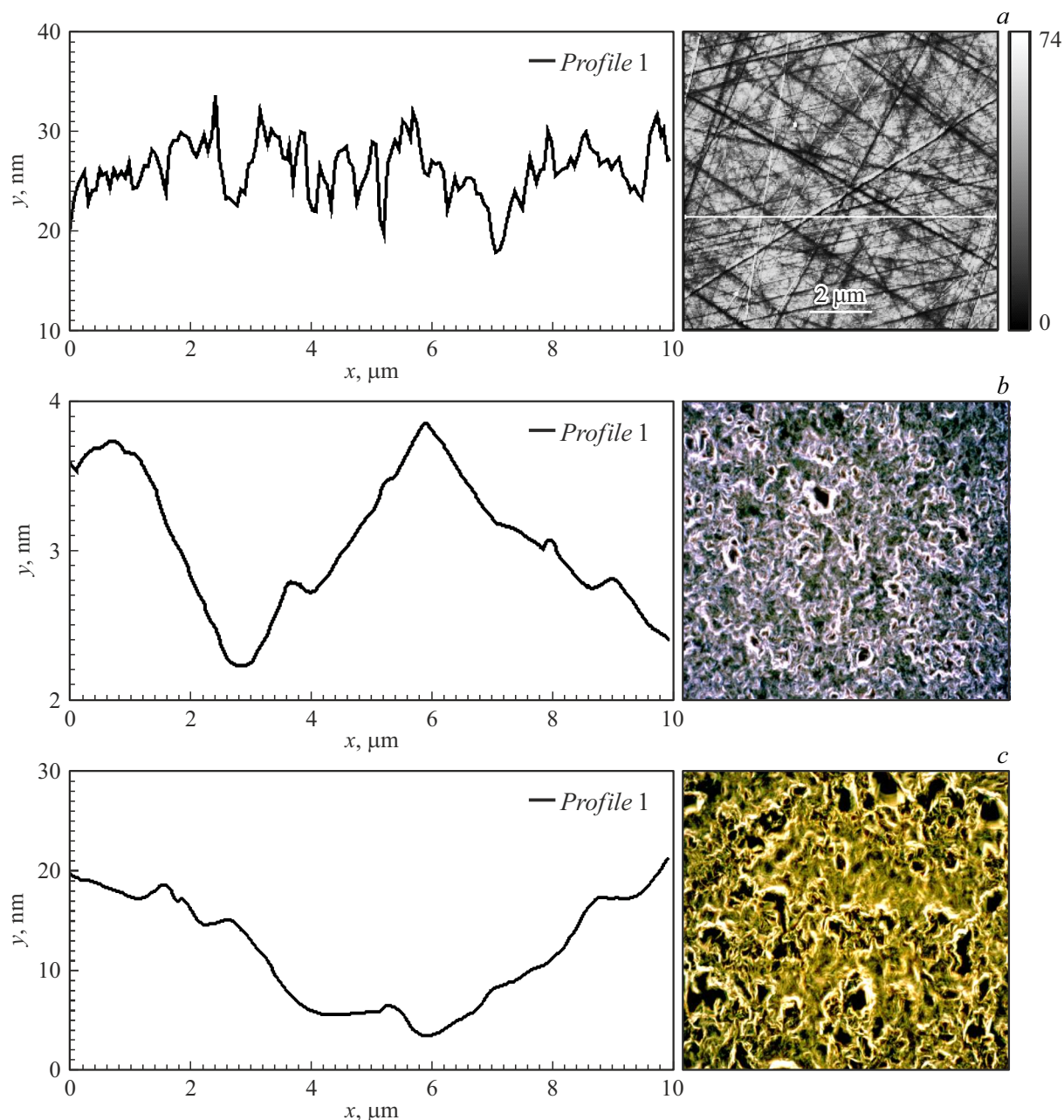
Figure 5. Typical profilograms and surface appearance for samples of group 7 polished with diamond paste with grain size $1\,\mu m$ (a), and samples of groups 8 and 9, ground with SiC powders with grain size 7 (b) and $14\,\mu m$ (c).

Table 5. Characteristics of the power spectrum of the random process of occurrence of irregularities on the surface of silicon wafers after CMP

Type of processing	Exponent n	Hurst constant H_1
CMP-1	1.28 ± 0.14	0.14 ± 0.07
CMP-2	1.90 ± 0.13	0.46 ± 0.07

persistence, i.e., the growth of the observed value is replaced by a decrease and vice versa. It can be assumed that the closer the Hurst index is to 0.5, the greater is the deviation from periodicity and the process is closer to chaotic. Thus, a less ordered distribution of the heights of the relief of the plate surface contributes to an increase in strength. Perhaps this is attributable to the fact that the randomness of the relief makes it difficult for the origin and development of near-surface cracks in the sample. This conclusion is important because, along with strength measurements, it can be used to predict the service life of plates.
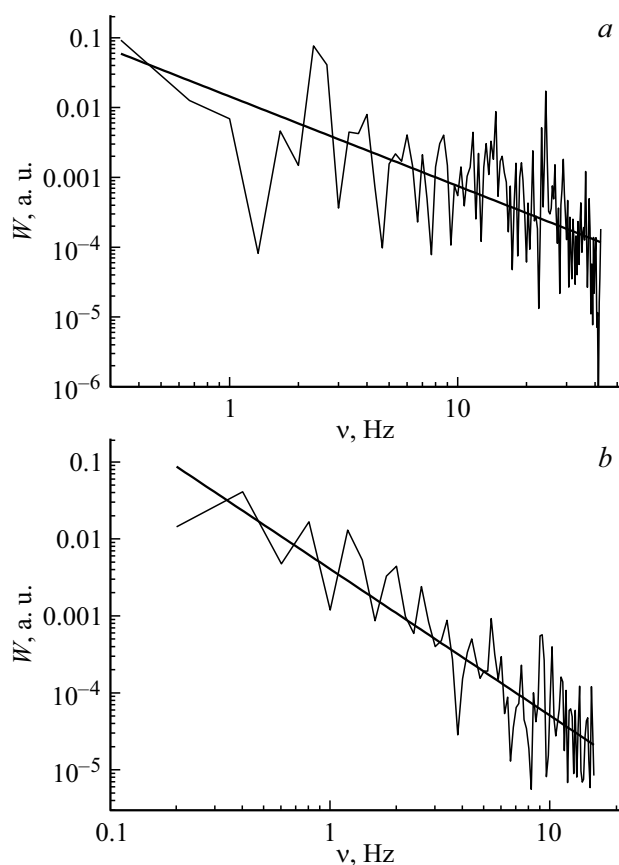
Figure 6. The dependence of the real part of the power spectrum of the random process of occurrence of micro-irregularities on the silicon surface presented in double logarithmic coordinates (Fig. 3), the type of finishing treatment: CMP-1 (*a*), CMP-2 (*b*).

Conclusion

1. The surface condition of thin silicon wafers is the most important factor determining their strength. The impact of the conditions for obtaining and processing thin silicon wafers on their strength was addressed in the papers listed above [1−16]. Any change in these conditions, even such as the place in the plate in the ingot from where it was cut, the alloying of the plate material with controlled or background impurities, the location of a small chip on an initially large plate affect the strength of the sample. However, the main impact on the strength of thin and ultrathin plates is exerted by the modes of their mechanical and chemical-mechanical processing. Moreover, in order to achieve maximum strength, the decisive factor is the choice of optimal conditions for finishing the CMP, ensuring smooth surfaces with a minimum level of roughness. The implementation of such conditions is possible when using a two-stage CMP with lapping, minimizing the mechanical component of the material removal process.

2. When determining the strength of brittle thin plates, in addition to the problems associated with the correct preparation of test samples, there are equally important problems of choosing the test method and calculating the strength. Biaxial bending tests should be used to avoid the impact on the strength of the edge effect present in the uniaxial bending test. Strength calculations based on the formulas of the theory of elasticity for thin plates are valid only for low-strength samples, and therefore are not of particular interest. The FEM method allows calculating the strength according to existing programs for modeling the bending process of the plate, but in order to assess the correctness of the chosen model, it is necessary to develop methods for its experimental verification. In the first approximation, it is possible to assess the validity of the computational model by comparing the experimental dependence of the deflection of the plate with the obtained using FEM.

3. In addition to the problems listed above related to the methods of preparing thin plates and determining their strength limit, there is a problem of choosing the right key quantitative characteristics of the morphology of the surface of the plates that determine their strength, methods of their registration and processing. In this paper, the surface profile of silicon wafers is measured and an attempt is made to link the strength of silicon wafers with standard surface roughness characteristics (GOST 2789−73, ISO 25178). It is shown that even a small change in the surface state depending on the CMP mode (CMP-1 or CMP-2) has a decisive effect on the strength of the plates. An explanation has been proposed linking this result with the influence of chemical polishing prevailing in CMP-2, which smooths out irregularities by reducing their height and stretching the irregularities over a longer surface length. At the same time, it was possible to associate the strength of the samples with the parameters of their surface for various modes of CMP only using the results of accurate measurements performed using an atomic force microscope with a subnanometer resolution.

4. When estimating the uptime of devices based on thin silicon wafers, based on predicting possible changes in the mechanical properties of wafers and their destruction, it is necessary to take into account not only the average static strength and structure of the surface profile, but also possible kinetic effects, since with cyclic and pronounced dynamic loading of thin wafers, the probability of failure it turns out to be significantly higher than with static exposure.

Conflict of interest

The authors declare that they have no conflict of interest.

References

[1] F. Kaule, B. Köhler, J. Hirsch, S. Schoenfelder, D. Lausch. Sol. Energy Mater. Sol. Cells, **185**, 511 (2018). DOI: 10.1016/j.solmat.2018.05.057

[2] V.A. Popovich, A. Yunus, M. Janssen, I.M. Richardson, I.J. Bennett. Sol. Energy Mater. Sol. Cells, **95**, 97 (2011). DOI: 10.1016/j.solmat.2010.04.038

[3] V.A. Popovich, A.C. Riemslag, M. Janssen, I.J. Bennett, I.M. Richardson. Int. J. Mater. Sci., **3**, 9 (2013).

[4] H. Sekhar, T. Fukuda, K. Tanahashi, H. Takato, H. Ono, Y. Sampei, T. Kobayashi. Mater. Sci. Semicond. Process., **119**, 105209 (2020) DOI: 10.1016/j.mssp.2020.105209

[5] J.-H. Woo, Y.-Ch. Kima, S.-H. Kima, J. Jang, H. N. Hanc, K.J. Choi, I. Kim, J.-Y. Kima. Scripta Mater., **140**, 1 (2017). DOI: 10.1016/j.scriptamat.2017.06.047

[6] M. Boniecki, P. Kamiński, W. Wesołowski, K. Krzyżak. Maerialityte-Elektrniczne (Electron. Mater.), **44**, 8 (2016).

[7] D. Echizenya, H. Sakamoto, K. Sasaki. Proced. Eng., **10**, 1443 (2011). DOI: 10.1016/j.proeng.2011.04.239

[8] A.M. Gabor, R. Janoch, A. Anselmo, J.L. Lincoln, H. Seigneur, Ch. Honeker. *Proc. of the IEEE 43rd Photovoltaic Specialists Conf (PVSC)* (Portland, OR, USA, 2016), v. 6.1, p. 3574. DOI: 10.1109/PVSC.2016.7750338

[9] S. Gouttebroze, H.I. Lange, X. Ma, R. Glockner, B. Emamifard, M. Syvertsen, M. Vardavoulias, A. Ulyashin. Phys. Status Solidi A, **210**, 777 (2013). DOI: 10.1002/pssa.201300003

[10] G. Coletti, N. van der Borg, S. De Iuliis, C.J.J. Tool, L.J. Geerligs. *Proc of the 21st European Photovoltaic Solar Energy Conference and Exhibition* (Dresden, Germany, 2006), rx06032.

[11] V.A. Popovich, W. Geerstma, M. Janssen, I.J. Bennett, I.M. Richardson. *EPD Congress 2015*. Ed. by J. Yurko, A. Allanore, L. Bartlett, J. Lee, L. Zhang, G. Tranell, Y. Meteleva-Fischer, S. Ikhmayies, A.S. Budiman, P. Tripathy, G. Fredrickson (Springer, 2016), 241−248.

[12] E. Cereceda1, J. Barredo, J.R. Gutierrez, J.C. Jimeno. *Proc. of the 25th European Photovoltaic Solar Energy Conference and Exhibition. 5th World Conference on Photovoltaic Energy Conversion* (Valencia, Spain, 2010), 1665−68.

[13] V.V. Shpeizman, V.I. Nikolaev, A.O. Pozdnyakov, A.V. Bobyl', R.B. Timashov, A.I. Averkin. Tech. Phys. **65** (1), 73 (2020). DOI: 10.1134/S1063784220010259

[14] S.E. Nikitin, V.V. Shpeizman, A.O. Pozdnyakov, S.I. Stepanov, R.B. Timashov, V.I. Nikolaev, E.I. Terukov, A.V. Bobyl. Mater. Sci. Semicond. Process., **15**, 106386 (2022). DOI: org/10.1016/j.mssp.2021.106386

[15] G. Rozgonyi, K. Youssef, P. Kulshreshtha, M. Shi, E. Good. Solid State Phenomena, **178**–**179**, 79 (2011). DOI: 10.4028/www.scientific.net/SS. P. 178−179.79

[16] A. Masolin, P. Bouchard, R. Martini, M. Bernacki. J. Mater. Sci., **48**, 979 (2013). DOI: 10.1007/s10853-012-6713-7

[17] F.F. Wittman, V.P. Pukh. Zavodskaya laboratoriya, **29**, 863 (1963) (in Russian).

[18] M. Oswald, T. Loewenstein, O. Anspach, J. Hirsch, D. Lausch, S. Schoenfelder. *Proc of the European PV Solar Energy Conference and Exhibition* (Amsterdam, Netherlands, 2014). DOI: 10.4229/EUPVSEC20142014-2AV.1.38

[19] M. Staudacher, T. Lube, J. Schlacher, P. Supancic. Open Ceramics, **6**, 100101 (2021). DOI: 10.1016/j.oceram.2021.100101

[20] W. Weibull. J. Appl. Mech., **18**, 293 (1951). DOI: 10.1115/1.4010337

[21] V.A. Stepanov, N.N. Peschanskaya, V.V. Speizman. *Prochnost' i relaksacionnye yavleniya v tverdykh telakh* (Nauka, L., 1984), 245 p. (in Russian).

[22] N.I. Kargin, A.S. Gusev, S.M. Ryndya, A.D. Bakun, A.E. Ieshkin, A.A. Akovantseva, P.I. Misurkin, S.G. Lakeev, I. Matushchenko, S.F. Timashev. Sci. Vis., **9**, 28 (2017).

[23] M. Zaiser. Adv. Phys., **55**, 185−245 (2006).

[24] J. Feder. *Fractals* (Plenum Press, NY., 1988)

[25] E. Bouchaud. J. Phys. Condens. Matter., **9**, 4319 (1997). DOI: 10.1088/0953-8984/9/21/002

[26] V.A. Oborin, M.V. Bannikov, Y.V. Bayandin, M.A. Sokovikov, D.A. Bilalov, O.B. Naimark. PNRPU Mech. Bull., **2**, 116 (2015). DOI: 10.15593/perm.mech/2015.2.07

[27] S.F. Timashev, Yu.S. Polyakov. Fluct. Noise Lett., **7**, R15 (2007). DOI: 10.1142/S0219477507003829

[28] S.D. Andreev, L.S. Ivlev. Optika atmosfery i okeana, **10**, 1450 (1997) (in Russian).

Translated by A.Akhtyamov